



HAL
open science

SANS study of structural changes in irradiated FeCu dilute alloys

M.-H. Mathon, F. Maury, F. Dunstetter, N. Lorenzelli, C.-H. de Novion,
François Boué

► **To cite this version:**

M.-H. Mathon, F. Maury, F. Dunstetter, N. Lorenzelli, C.-H. de Novion, et al.. SANS study of structural changes in irradiated FeCu dilute alloys. *Journal de Physique IV Proceedings*, 1993, 03 (C8), pp.C8-279-C8-282. 10.1051/jp4:1993854 . jpa-00252285

HAL Id: jpa-00252285

<https://hal.science/jpa-00252285v1>

Submitted on 4 Feb 2008

HAL is a multi-disciplinary open access archive for the deposit and dissemination of scientific research documents, whether they are published or not. The documents may come from teaching and research institutions in France or abroad, or from public or private research centers.

L'archive ouverte pluridisciplinaire **HAL**, est destinée au dépôt et à la diffusion de documents scientifiques de niveau recherche, publiés ou non, émanant des établissements d'enseignement et de recherche français ou étrangers, des laboratoires publics ou privés.

SANS study of structural changes in irradiated FeCu dilute alloys

M.-H. MATHON, F. MAURY, F. DUNSTETTER, N. LORENZELLI, C.-H. DE NOVION and F. BOUÉ*

Laboratoire des Solides Irradiés, CEA/CEREM, Ecole Polytechnique, 91128 Palaiseau cedex, France

** Laboratoire Léon Brillouin, CE Saclay, 91191 Gif sur Yvette cedex, France*

Abstract: Copper-rich precipitates formed in iron based dilute alloys by irradiation or thermal ageing, have been investigated using small angle neutron scattering (SANS). In particular, FeCu1.5% has been studied after either 2.5 MeV electron irradiations at 300°C or thermal ageing at 500°C. Size distribution, composition and number density of the clusters were deduced from SANS data. In addition, microhardness measurements allowed to correlate precipitates configuration with alloys hardening. The precipitation mechanism looks the same for both kinds of ageing, but irradiation induces an additional contribution to hardening. A linear correlation between duration of thermal ageing and irradiation fluence can be established.

INTRODUCTION

It is well known that copper-rich clusters play a significant role in the embrittlement process of reactor pressure vessel steels /1-3/. As a matter of fact, copper precipitates which are created during neutron irradiation at 290°C induce hardening and embrittlement by pinning the dislocations.

With the aim of understanding the copper precipitation mechanisms under irradiation, we have studied this phenomenon in binary dilute FeCu model alloys irradiated with 2.5 MeV electrons in the 175-360°C temperature range. Electron irradiation has been chosen for its efficiency since most of the created point defects participate in long range atomic motion, producing an acceleration of the copper precipitation. In order to compare the precipitation mechanisms, the same alloys were thermally aged at 500°C.

Precipitation under irradiation was monitored by resistivity measurements /4/ and was characterized by small angle neutron scattering experiments (SANS). Finally, microhardness measurements gave complementary information about the hardening of the alloys.

EXPERIMENTAL

-Materials:

The studied materials are binary alloys containing from 0.1 to 1.5% Cu, in an α -Fe-matrix. After being cold-rolled, the samples are quenched after a 24h annealing in the b.c.c. solid solution phase (820°C) in order to get low dislocation density and a good homogeneity.

-Irradiation:

The samples were irradiated with 2.5 MeV electrons under helium atmosphere at fluences up to $5C/cm^2$. The samples were heated with the electron beam up to temperatures in the range of 170 to 360°C. The kinetics of precipitation under irradiation has been monitored "in situ" by measuring the electrical resistivity at 30°C at regular dose intervals. Assuming the precipitates do not contribute to the resistivity, the decrease of this parameter can be related to copper depletion of the matrix /4/.

-SANS experiments:

SANS experiments were performed at the Laboratoire Léon Brillouin (CEA-CNRS), CE Saclay, on the PAXY spectrometer, at room temperature under saturating magnetic field H (1.4 T) with neutrons of 0.6 nm wavelength. The two-dimensional position sensitive detector was placed at 3.28 m from the sample, covering a scattering vector range up to 1.2 nm^{-1} .

SANS INTERPRETATION

SANS intensity is composed of a nuclear and a magnetic contribution which depend respectively on the difference of composition and of magnetization between the precipitates and the matrix. In terms of cross section, SANS intensity can be written as:

$$\left(\frac{\partial\Sigma}{\partial\Omega}\right)(q, \alpha) = f(1-f)\left[(\Delta\eta)_{nucl}^2 + (\Delta\eta)_{mag}^2 \sin^2 \alpha\right]F(q, h(R), S(q, R))$$

where q is the scattering vector, α the angle between the scattering vector and the magnetization of the sample, f the precipitated atomic fraction, $(\Delta\eta)_i^2$ the contrasts, and $F(q, h(R), S(q, R))$ the specific structure factor of the scattering particles, depending on the size distribution $h(R)$ and the form factor $S(q, R)$.

Assuming that precipitates are non-ferromagnetic and that precipitate and matrix densities are approximately the same, the nuclear (nucl) and magnetic (mag) contrasts become proportional to the average scattering length (\bar{b}) variation between the precipitates (p) and the matrix (m):

$$(\Delta\eta)_{nucl}^2 \propto (\bar{b}_{nucl}^p - \bar{b}_{nucl}^m)^2 \quad \text{and} \quad (\Delta\eta)_{mag}^2 \propto (-\bar{b}_{mag}^m)^2$$

Here, $\bar{b}_{mag}^m = (\gamma_0/2)\mu_{Fe}$, where $\gamma_0 = -1.913$ is the gyromagnetic factor of the neutron, $r_0 = 0.2818 \cdot 10^{-14} m$ is the classical electron radius and μ_{Fe} is the magnetic moment of iron.

The scattering intensities, measured in directions parallel and perpendicular to the sample's magnetization, allow the determination of clusters composition. In fact, the A ratio defined as:

$$A = \left(\frac{\partial\Sigma}{\partial\Omega}\right)_\perp / \left(\frac{\partial\Sigma}{\partial\Omega}\right)_\parallel \approx 1 + \bar{b}_{mag}^m / (\bar{b}_{nucl}^p - \bar{b}_{nucl}^m)$$

depends only on the precipitates composition. In this expression, we neglect a less than 0.2% magnetic contribution to the experimental parallel cross section.

The precipitated fraction f can be easily determined if the composition and the structure factor of the clusters are known. The structure factor depends on a form factor $S(q, R)$ and on the size distribution of the particles $h(R)$. The precipitates are assumed to be spherical with radius R , and without spatial correlations. Such assumptions lead to the well-known form factor:

$$S(q, R) = \left[3(\sin qR - qR \cos qR) / (qR)^3\right]^2$$

Concerning $h(R)$, several (empirical) distributions have been tested and the best fit to the experimental data was obtained with a gaussian distribution. On the other hand, the Lifshitz-Slyozov-Wagner theory (LSW) based on thermodynamical nucleation-growth-coarsening models gives two distributions depending on the growth kinetics model considered [5-7]. These distributions, depending on only one fitting parameter $\rho = R/\bar{R}$, where \bar{R} is the mean radius of the clusters, are given respectively by :

$$h(\rho) \propto \rho^2 \left[3/(3+\rho)\right]^{7/3} \left[1.5/(1.5-\rho)\right]^{11/3} \exp[-\rho/(1.5-\rho)] \quad (\text{LSW1})$$

if the growth kinetics is diffusion controlled, and by :

$$h(\rho) \propto \rho \left[2/(2-\rho)\right]^5 \exp[-3\rho/(2-\rho)] \quad (\text{LSW2})$$

if the growth kinetics is interface-reaction controlled.

The LSW1 distribution is asymmetrical (Fig 1) and fits the data only at low fluences or ageing times. At the opposite, the LSW2 distribution, which is quasi-symmetrical, leads to very good agreement with experimental data at high ageing. In other words, the precipitates obey to a symmetric distribution above a given size.

Remark: In the literature, the logarithm normal distribution is frequently used but its asymmetry is at the opposite of that of LSW1 distribution. It has no physical bases and good fits to the data could not be obtained.

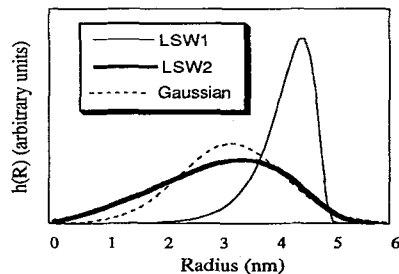


Fig 1: Gaussian and LSW's distributions for a FeCu1.5% irradiated 4.7 C/cm² at 300 °C .

RESULTS AND DISCUSSION

1) FeCu1.5% irradiated at 300°C:

The resistivity decreases very fast during the early stages of irradiation up to 0.5 C/cm^2 and tends toward an equilibrium value close to the pure- α -iron resistivity (fig 2a). This decrease results from copper depletion in the matrix and can be interpreted in terms of pure growth of precipitates, followed by coarsening in the saturation domain. Additionally, SANS studies show that the mean radius of the clusters increases with the fluence and this increase is faster at lowest fluences (fig 2-c). The precipitates number decreases (fig 2-d) but the experimental errors at low fluences prevent a precise determination of the precipitated atomic fraction; nevertheless, the coarsening seems to start before the resistivity saturation. This early coarsening is in agreement with previous results of Kampmann and Wagner /8/ on thermally aged iron-copper alloys.

The A ratio will be discussed later in the fourth paragraph.

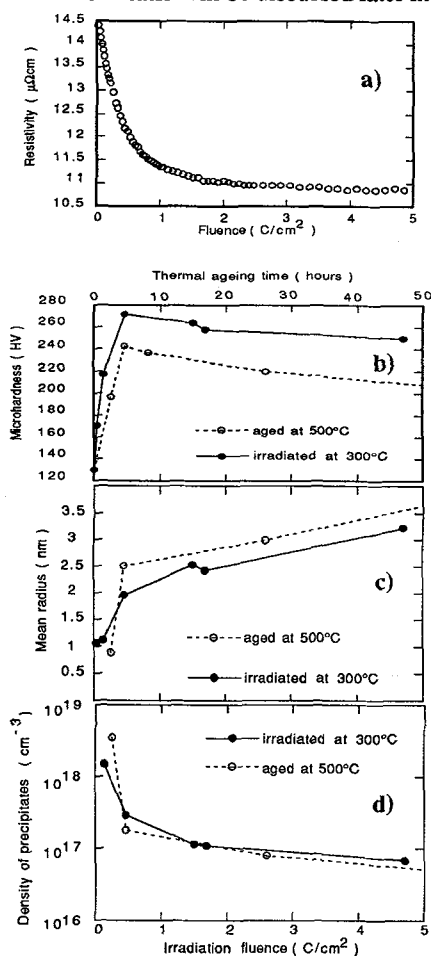


Fig 2: Variations of : (a) electrical resistivity ($\mu\Omega\text{cm}$), (b) microhardness (HV), (c) average size (nm) and (d) number of precipitates, with fluence for FeCu1.5% samples irradiated at 300°C and with time for FeCu1.5% samples thermally aged at 500°C. The SANS data were fitted with a gaussian model.

The Vickers microhardness was measured as a function of the fluence (fig 2-b). Our results show that the microhardness increases until a maximum around 0.5 C/cm^2 , and then decreases slightly. The microhardness behaviour can be associated to the pinning efficiency by the precipitates distribution. Concerning this point, it is well known /3/ that the precipitate number and their size play an important role in the optimization of pinning.

2) FeCu1.5% thermally aged at 500°C

The microhardness behaviour obtained after thermal ageing is similar to that of irradiated samples. Nevertheless, one of the main differences between these two types of ageings is the microhardness maximum value: the microhardness is higher for the irradiated case (fig 2-b). This point has been observed by other authors who compared thermal ageing and neutron irradiation /9/. This suggests the existence of an additional hardening mechanism under irradiation, such as the formation of point defect clusters not detected with SANS, although no hardening has been induced by 2 C/cm^2 irradiation in pure α -iron /10/.

3) Irradiation fluence versus thermal ageing time

For each of the various experimental results obtained (size and number of the precipitates, microhardness), the shape of the curves as a function of ageing parameter (time or fluence) is similar (fig 2-bcd). Furthermore, we have been able to establish a linear connection between thermal ageing time and irradiation fluence, which matches nearly exactly the characteristics of precipitates together with the position of the maximum of hardness. This indicates that, for a given temperature, the main effect of irradiation is an acceleration of precipitation (by point defect creation) with respect to thermal ageing at the same temperature. This is one of the assumptions of the theory developed by Smetniansky and Barbu /11/. It predicts the apparition of coarsening later than the experimental results.

4) Evolution of A ratio

The A ratio exhibits the same kind of evolution in both cases of irradiation at 300°C and thermal ageing at 500°C. In this latter case, we observe first an increase at short ageing times (from A=7 for 2h30 to A=10 for 4h30), then a slow decrease at long ageing times (down to A=7.5 for 312h).

We can expect the origin of this A variation to be distinct at first and late stages. It is difficult to estimate what could happen at first stages, due to the poor statistics arising from very small particles out of the SANS range. At late stages, the observed decrease of the A factor can be ascribed to an apparent decrease of the atomic density of the copper precipitates. The discrepancy between copper and iron atomic density is too low to explain such an effect and other mechanisms must be accounted for. Two mechanisms associated to a crystallographic transition of the copper phase, can be proposed: (1) a variation of density at the interface of the copper clusters and the iron matrix, (2) a variation of the density of the bulk of the precipitates themselves.

The small precipitates are coherent with the bcc cell of the iron matrix. At higher cluster size, the bulk free energy is optimized by a transition to the normal fcc copper structure /12/. Within model (1), the result is a misfit at the cluster-matrix interfaces; within model (2), we need a very high vacancy density. This seems doubtful and we prefer an interpretation in terms of interface misfit.

If such a mechanism is confirmed for thermal ageing, we can expect it to remain valid in the irradiation case.

CONCLUSIONS

The SANS experiments allowed to characterize the copper precipitates as a function of fluence or ageing time, and to evidence the quasi-symmetrical shape of the clusters size distribution.

The microhardness maximum value corresponds to a configuration where the precipitates are large and numerous enough to pin strongly the dislocations. At this stage, the precipitates seem to be composed only of copper.

We have been able to establish a linear correlation between the thermal ageing time and the fluence of 2.5MeV electrons at 300°C.

The irradiation induces an accelerated copper diffusion but the comparison of microhardness values between the different types of ageing shows that the hardening is not only the result of copper precipitation. Probably, point defect clusters also contribute to hardening.

Further developments are in progress with other alloys containing Ni, Mn, Cr... in order to understand the effect of additional elements on copper precipitation and hardening. Preliminary results show an important role of Mn on the kinetics of Cu precipitation /13/.

Acknowledgements.

We would like to thank A. Barbu for helpful discussions, J.C. Bisson for technical assistance for samples preparation, A. Brûlet and L. Noirez for their assistance during the SANS experiments.

References:

- /1/ Van Duysen J.C., EDF Report, HT-41/PV D 724-A, 1990, EDF Les Renardières, 77250 Moret-sur-Loing, France
- /2/ Odette G.R., Scripta Met., 1983, **17**, 1183
- /3/ Russel K.C., Brown L.M., Acta Met., 1972, **20**, 969
- /4/ Lê T.N., Barbu A., Liu D., F. Maury, Scripta Met., 1992, **26**, 771-776
- /5/ Martin G., in "Solid State Phase Transformation in Metals and Alloys", Aussois 1978, Les éditions de Physique, Orsay(1980), p.337
- /6/ Lifshitz I.M., Slyozov V.V., J. Phys. Chem. Solids, 1961, **19**, 35-50
- /7/ Wagner C., Z. Elektroch., 1961, **65**, 581
- /8/ Kampmann R., Wagner R., Atomic transport and defects in metals by neutron scattering, SPP **10**, Springer Verlag, Berlin, 1986, 73-77
- /9/ Buswell J.T., English C.A., Hetherington M.G., Phythian W.J., Smith G.D.W. and Worrall G.M., ASTM Andover, 1987
- /10/ Barbu A., Lê T.N., Lorenzelli N., Maury F. and de Novion C.H., Materials Science Forum **1992**, **97-99**, 351-358
- /11/ Smetniansky-de-Grande N., and Barbu A., to be published
- /12/ Pizzini S., Roberts K.J., Phythian W.J., English C.A. and Greaves G.N., Phil Mag. Lett., 1990, **61**, 223
- /13/ Maury F., Lorenzelli N. and de Novion C.H., 1991, J. of Nucl. Mat., **183**, 217-220